Ratio of Atomic Stopping Power of Graphite and Diamond for 1.1-Mev Protons*

SHELDON D. SOFTKY
Stanford Research Institute, Menlo Park, California
(Received March 14, 1961)

The theory describing energy loss of heavy charged particles in matter predicts that different physical or chemical forms of the same element will have slightly different stopping powers. Since two different forms of a pure element exhibit the same nuclear scattering cross section, it has been possible to measure the relative atomic stopping power of graphite and diamond by observing the yields of back-scattered protons from thick targets. The atomic stopping power of graphite has been measured to be 1.0604±0.0090 times that of diamond (for 1.1-Mev protons). Using the theoretical density of graphite, a calculation based on this result and Brandt's version of stopping theory yields the result that the molecular polarizability of graphite is 4.9 times that of diamond. If this calculation is made using the measured density of graphite, this polarizability ratio is 1.5, in agreement with the theoretical value.

INTRODUCTION

THE Bethe-Bloch theory of atomic stopping power[1–3] gives the rate of energy loss of heavy charged particles passing through an absorber as

$$-\frac{dE}{dx}=\frac{4\pi z^2e^4n}{mV^2}\left\{\ln\frac{2mV^2}{\bar{I}}-f(\beta^2)\right\}\ (\text{erg cm}^{-1}),$$

where V=velocity of the heavy particle, z=charge of the heavy particle, n=electron density of the absorber, $\beta=V/C$, and $\bar{I}$=the mean ionization potential of the substance. To a first approximation, the energy loss per unit target thickness occurs as the heavy particles collide with absorber electrons and depends only on the absorber's mean electron density. To the extent that the absorber can be regarded as a collection of isolated atoms, its physical or chemical state can be disregarded; and the stopping power of a mixture of elements would be the same as that of a compound with the same atom ratio.

However, recent development of the theory to take account of atomic interactions[4–6] has shown that three distinct effects upon stopping power exist which depend upon the chemical and physical state of the absorber. These effects are: (1) the valence effect, due to differences in strength of chemical binding energies of electrons of the absorber. The quantity $\bar{I}$ in the Bethe-Bloch equation takes account of this effect; (2) the longitudinal or zero-energy polarization which depends upon the polarization of the absorber by particles with relatively low velocity; and (3) the transverse or energy-dependent polarization, which depends on the crystalline nature of the absorber and its interaction with relativistic particles.

The Bethe-Bloch formula for stopping power is valid for particle velocities substantially higher than those of the electrons in the absorber; the energy-dependent polarization effect is negligible for all but very relativistic particles, and consequently has not been measurable in experiments on the stopping power of heavy particles.

Brandt[7] recently made extensive calculations of the stopping powers of molecular compounds for non-relativistic particles. These calculations predict atomic binding effects of up to 2% of the total stopping power. The theory relating the valence effect to stopping power has been tested in experiments of Thompson[8] and of Bakker and Segrè[9] with 340-Mev protons, and of Caldwell[10] with 10- to 20-Mev protons. Within their errors, the results of these experiments agree with theory, but none of these experiments directly compares the stopping powers of different physical forms of a single atomic species.

The original intent of the present experiment was to investigate the valence effect by measuring the difference in stopping power between an insulator and a conductor which are identical in atomic composition. Since the theory predicts the greatest difference in this case for the substance with the highest fraction of valence electrons, graphite, and diamond with four valence electrons were convenient and adequate for the comparison. The same experiment can obviously be done with any element (or compound) which has allotropic forms. The major experimental requirement for the use of allotropes in this experimental method is that surfaces of good metallurgical polish of $\frac{1}{4}$ in. diam be obtainable on the solid substances of interest.

THEORETICAL BASIS FOR THE EXPERIMENT

An accurate direct determination of the stopping power of a substance can be made using an absorber of accurately known thickness that is thin relative to

* Work supported by the Division Research Committee of the Physical and Life Sciences Division, Stanford Research Institute.
[1] N. Bohr, Phil. Mag. **25**, 10 (1913); N. Bohr, Phil. Mag. **30**, 581 (1915).
[2] H. Bethe, Ann. Physik **5**, 325 (1930).
[3] F. Bloch, Z. Physik **81**, 363 (1933).
[4] E. Fermi, Phys. Rev. **56**, 1242 (1939).
[5] O. Halpern and H. Hall, Phys. Rev. **57**, 459 (1940); **73**, 477 (1948).
[6] R. M. Sternheimer, Phys. Rev. **88**, 851 (1952); **103**, 511 (1956).
[7] W. Brandt, Phys. Rev. **104**, 691 (1956); **105**, 1933 (1957).
[8] T. Thopmson, Ph.D. thesis, University of California, Berkeley, California, 1952 (unpublished).
[9] C. Bakker and E. Segrè, Phys. Rev. **81**, 489 (1951).
[10] D. Caldwell, Phys. Rev. **100**, 291 (1955).

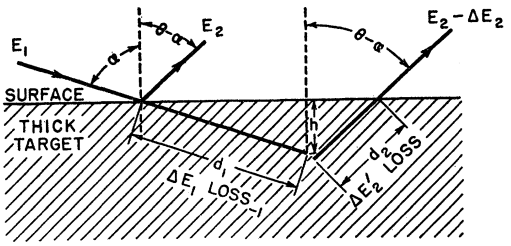

FIG. 1. Geometry for scattering.

the range of the beam particles. This method is limited to high energy particles and its accuracy limited by the poor energy stability of high energy accelerators.

However, it is possible to determine the stopping power of substances not available in thin films, since the yield of protons scattered from the surface of a thick target is dependent upon the stopping power of the target as well as its scattering cross section. In the method of analyzing scattered protons, described by Brown *et al.*[11] the scattered protons are counted after traversing a magnetic spectrometer. For elastic scattering,

$$E_2=kE_1, \tag{1}$$

where E_2 is the energy of the scattered proton and k is determined by the target atom mass, M, and by the angle between the incident and scattered protons, θ. Figure 1 shows the scattering schematically. The target is assumed to be isotropic and homogeneous. The measured yield, C, is given by (see Appendix for proof.)

$$C=\frac{2E_1\sigma q\Omega}{R_s}\left[\epsilon_1+\frac{\cos\alpha}{\cos(\theta-\alpha)}\frac{\epsilon_2}{k}\right]^{-1}, \tag{2}$$

where ϵ_1=the target's atomic stopping power for protons before scattering, ϵ_2=the target's atomic stopping power after scattering, σ=the differential scattering cross section at the incident energy E_1, q=the number of incident protons, Ω is the acceptance solid angle, R_s is the momentum resolution of the spectrometer, and α is the angle between the normal to the target face and the incident beam direction.

By interchanging graphite and diamond targets while holding all other experimental parameters constant, the scattering yields of graphite, C_g, and diamond, C_d, are measured.

By dividing Eq. (2) for graphite by Eq. (2) for diamond, the ratio of the stopping powers of the two targets can be written

$$\frac{\epsilon_{g1}}{\epsilon_{d1}}=\frac{C_d}{C_g}\left[1+\frac{r_d}{k}\frac{\cos\alpha}{\cos(\theta-\alpha)}\right]\Big/\left[1+\frac{r_g}{k}\frac{\cos\alpha}{\cos(\theta-\alpha)}\right], \tag{3}$$

where

$$r_d=\epsilon_{d2}/\epsilon_{d1}, \quad r_g=\epsilon_{g2}/\epsilon_{g1}. \tag{4}$$

[11] A. Brown, C. Snyder, W. Fowler, and C. Lauritsen, Phys. Rev. **82**, 159 (1951).

Protons scattered at 90° from carbon have 85% of their initial energy (i.e., $k=0.85$). For this 15% change in energy, the theory of the valence effect on energy loss predicts that $r_g-r_d<0.01$. Furthermore in the experimental arrangement used, $\theta=90°$ and $\theta-\alpha=15°$, so that $\cos\alpha/\cos(\theta-\alpha)=0.27$.

Series expansion of (3) shows that the approximation

$$\epsilon_{g1}/\epsilon_{d1}\simeq C_d/C_g \tag{5}$$

is in error by less than 0.3%, or less than the probable error of the experiment, and will not be affected by expected errors in θ and α.

EXPERIMENTAL PROCEDURE

The proton beam of nominal energy 1.2 Mev was produced by a Van de Graaff accelerator. An analyzing magnet and energy stabilizing system held the beam energy constant to about three parts in 10^4. The accelerator was equipped with a quadrupole electrostatic lens with which the beam could be focused to a spot on the target smaller than 1 mm^2. A double-focusing 180° magnetic spectrometer with $R_s=1100$ was used to analyze the scattered protons. Figure 2 shows the arrangement of beam, target, and spectrometer.

The diamond was a gem-quality stone, of approximately two carats, with plane-parallel polished faces approximately $\frac{1}{4}$ in. square. It was cemented with Sauereisen cement into a matching hole in a Vycor plate, 0.450-in. square and $\frac{1}{8}$ in. thick, with the diamond surface accurately coplanar with one surface of the Vycor. The cement was not allowed to extrude on the target side of the stone, and the entire unit was examined under 25× magnification to be sure the surface was clean and that the periphery of the mount was not shadowing the target surface in any way.

Two graphite targets were used, of entirely different origin. The first was a piece of nuclear reactor graphite of density 1.57 g/cm^3 cut to a $\frac{3}{8}$-in.-diam screw, with the point polished flat by burnishing alternately with polished copper and a soft cloth. This graphite was

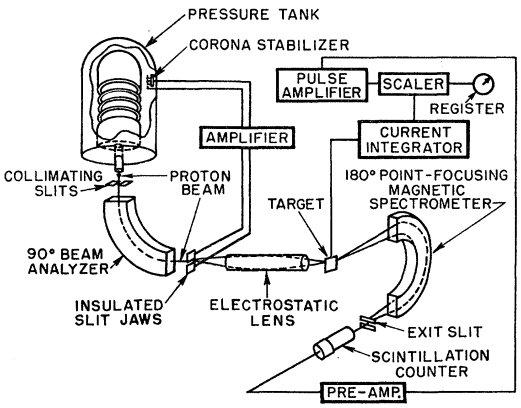

FIG. 2. Experimental arrangement.

screwed into the target holder until the polished end rested on the target holder surface. The second graphite target was pyrolytic graphite of density 1.78 g/cm³ formed on a polished Vycor disk by "cracking" propane at very low pressure at about 1200°C. The pyrolytic graphite surface formed on the Vycor was almost of mirror smoothness, even under 25× magnification. The graphite target was removed from the Vycor and glued by its edges into the target holder.

These three targets were mounted in a target holder and were placed coplanar to within 0.001-in. with a target angle error of less than 3 min of arc out of an angle of 15° with the beam. Targets were interchanged by moving the holder up and down with a shaft whose axis was coplanar with the targets to a tolerance of 0.002-in. A Vycor plate, also coplanar with the target surface, was attached to the target holder; and the beam was focused and positioned by observing its fluorescence on this plate.

The scattered protons were detected in the magnetic spectrometer by a CsI crystal 0.020 in. thick cemented to a 2-in. Lucite light pipe on a Du Mont 6292 photomultiplier tube. The output of this tube drove two scalers in parallel to obtain duplicate data collection. The output of the amplifier of one of the scalers was monitored on an oscilloscope which was also used to observe the pulse height to which the scalers were biased.

The scalers were manually turned on but automatically turned off by the beam current integrator after the accumulation of either 10 or 100 μcoul of integrated beam, as desired. The trigger level of this current integrator[12] was periodically checked with a $+10$ to -10 mv input. The integrator held the incident charge q constant to better than 3 parts in 10^4 for all measurements.

The target holder was surrounded by an insulated electrostatic shield with access holes for the incident beam and the scattered beam. This shield was connected to the target holder by a 900-v battery which biased the shield negative relative to the target. This potential suppressed secondary electron emission from the target and collected any positive ions sputtered from the target so that in neither case should secondary emission have seriously affected the precision of the current integration.

The experimental measurements consisted of (1) determination of the momentum spectrum of protons scattered from each of the three targets, and (2) determination of the relative scattering yields from each of the three targets at points where the momentum spectrum was flat.

The determination of the momentum spectrum of the target was essential to show that each target exhibited the same momentum spectrum and to show

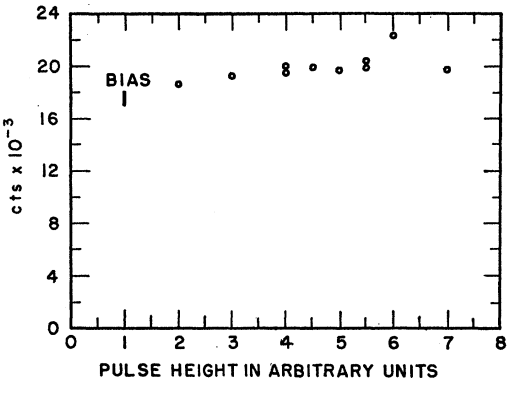

FIG. 3. Counting rate plateau.

that no protons were scattered from any material except the carbon of the targets. The ratio k in Eq. (1) of scattered proton energy to incident proton energy was determined only by the mass of the scattering nucleus and the scattering angle, θ. Due to this dependence on target nuclear mass, the most energetic scattered protons indicated the heaviest atoms present in the target. A measurement of the momentum spectrum constitutes an additional test of target purity from heavier elements, as well as an indication that all three targets are acting as smooth carbon surfaces for scattering.

The experiment was performed by setting the scaler thresholds at one-fifth the maximum pulse height due to scattered protons, after obtaining the counting rate plateau shown in Fig. 3, and then obtaining four counts for each target at each of two spectrometer current settings as shown in Table I. The column, C_d/C_g gives the ratio of actual numbers of counts accumulated per 100μ coul of protons. The momentum spectra were then obtained by counting each target for only 10 μcoul of beam at each magnet current setting, as shown in Figs. 4 and 5.

The limitation on accuracy of these measurements was undoubtedly due to instability of the scalers or of the high-voltage supply. The total number of counts used for the calculated ratios was nearly 3×10^6 each for diamond and graphite. Therefore, the statistical error of less than 0.1% is negligible compared to the observed experimental deviations.

A set of five consecutive counting measurements on the Vycor target with all conditions supposedly constant (for 100 μcoul of beam for each point) showed a standard deviation of about 0.5%. The standard deviation of a ratio based on two such sets of counts would be $\sqrt{2}\times0.5\%$ or about 0.7%. The observed standard deviation for 16 measurements of the diamond/graphite counting ratios was 0.9%. If the counting equipment (or the photomultiplier supply) had been more stable, early experimental work showed that sputtering of the target surfaces by the beam would have become the limitation on accuracy. About

[12] G. Bouricius and F. Shoemaker, Rev. Sci. Instr. 22, 183 (1951).

TABLE I. Measured ratios of stopping power for graphite and diamond targets.

Relative spectrometer current	Scaler	$C_d/C_{pyro}=\epsilon_{pyro}/\epsilon_{diam}$	$\lvert\Delta X\rvert$	$C_d/C_{reactor}=\epsilon_{reactor}/\epsilon_{diam}$	$\lvert\Delta X\rvert$
7.15	I	177 804/168 752=1.0533	0.0096	177 804/168 720=1.0539	0.0098
	I	179 456/167 691=1.0703	0.0074	179 456/167 484=1.0716	0.0079
	II	178 660/168 454=1.0605	0.0024	178 660/168 338=1.0618	0.0019
	II	178 979/167 676=1.0674	0.0045	178 979/167 663=1.0674	0.0037
		Mean[a]=1.0629±0.0066		Mean=1.0637±0.0067	
7.25	I	183 883/173 381=1.0606	0.0060	183 883/172 081=1.0686	0.0080
	I	182 123/171 738=1.0605	0.0060	182 123/173 067=1.0520	0.0080
	II	184 186/173 034=1.0647	0.0110	184 186/172 354=1.0691	0.0085
	II	181 902/176 188=1.0323	0.0220	181 902/172 781=1.0527	0.0080
		Mean=1.0545±0.0130		Mean=1.606 ±0.0082	

[a] Errors shown with the means are standard deviations.

1000 μcoul of beam on a 1-mm^2 spot on a graphite target was sufficient to cause its scattering counting rate to diminish erratically by 1% or more.

For the same irradiation a larger beam spot gave longer target life, but the 1-mm^2 spot was necessary to keep the beam spot on the plane polished surface of the diamond. The fluorescence of the beam spot on the diamond was carefully watched during every diamond scattering in order to be sure that all of the beam was accurately centered on the plane surface of the diamond. The graphite surfaces, being larger, did not require this attention. The agreement between the two graphite samples, despite apparent differences in smoothness, showed that the reactor graphite was smooth enough for adequate results.

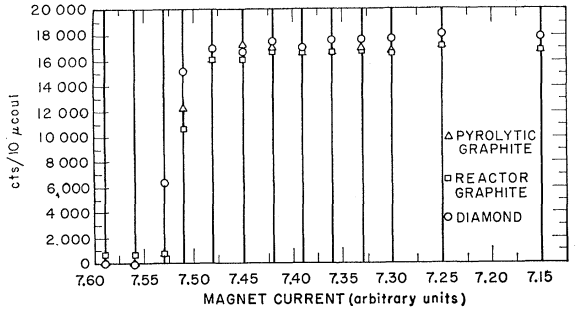

FIG. 4. Momentum spectra recorded by scaler I.

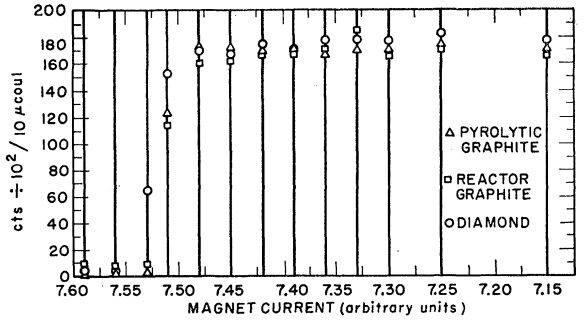

FIG. 5. Momentum spectra recorded by scaler II.

An electrostatic charge on the diamond could cause the effective beam energy to be lowered. To discourage the presence of such a charge, Aquadag was painted in a thin layer up to the edge of the plane target surface. Any voltage difference between the beam spot and the target holder would have to have been held across about 1 mm of the diamond surface, with a knife edge of Aquadag on the ground side. It is doubtful if more than a few kilovolts could be held across such a gap, and it would have been necessary to hold about 50 kilovolts to cause the incident energy to change enough to increase the scattering cross section of the diamond by 5%. In the dark no sparks were ever observed to jump from the beam spot to the edge of the diamond.

EXPERIMENTAL RESULTS

Ratio of Stopping Powers

Table I shows the ratio of diamond to graphite scattered proton yields for 100 μcoul of protons at two different values of spectrometer current as recorded by the two different scalers. The average ratios and standard deviations for each type of graphite at each magnet current setting are also given. The size of the errors permits these measurements to be lumped together, giving a single average and standard deviation of

$$C_d/C_g=\epsilon_g/\epsilon_d=1.0604\pm0.0090,$$

for protons at a nominal energy of 1.1 Mev as measured by the generating voltmeter of the accelerator, and as corrected for scattering depth in the target.

The momentum spectra of protons scattered from the three targets as measured by the two scalers are shown in Figs. 4 and 5. The ratios in Table I were obtained at the two lowest magnet current points on each curve. The agreement in shape of the momentum profiles for all three targets shows that contamination of target surfaces by N_2, O_2, H_2O, or heavier elements was not sufficient to affect the accuracy of the results outside of the counting fluctuations which are

apparent.[13] The agreement between yields and spectra for two types of graphite as different in density and origin as these were is strong evidence that contamination of the graphite could not have caused the observed difference in scattering yield between graphite and diamond. The difference in smoothness between the graphite and diamond surfaces could explain the slight difference between the momentum profile "edges" of graphite and diamond. However the difference in momentum profile "edges" was not large enough relative to the available momentum resolution to significantly affect results. The counting rate ratios used to obtain stopping power were obviously taken on a sufficiently flat part of the momentum spectrum to make the available stability and resolution of the spectrometer adequate.

Absolute Stopping Power of Graphite

An absolute value of the stopping power of graphite can be obtained using the absolute yield of protons scattered from graphite. The counting rate plateau shown in Fig. 1 is sufficiently flat that the counting error should be well under that quoted for most absolute cross sections. The constants of the spectrometer are known from previous work.[14] They appear in Eq. (2) as the laboratory solid angle Ω and R_s (momentum resolution) of the instrument. We can approximate

$$r_g = \epsilon_g(\text{after scattering})/\epsilon_g(\text{before scattering}),$$

from the data of Fuchs and Whaling,[15] as $r_g = 1.117$; and $k = 0.845$ for carbon-12 at $\theta = 90°$. The carbon-12 scattering cross section measured by Jackson *et al.*[16] can be extrapolated to a center-of-mass angle of 94.7° (90° lab angle). This cross section was measured using a gas target, and hence does not depend directly upon any known value of the carbon stopping power. Figure 6 shows the extrapolation used to obtain σ at $\theta = 90°$. The accuracy quoted by the author ($\pm 5\%$) is shown on the curve. From this extrapolation

$$\sigma(90° \text{ lab, } 1.1 \text{ Mev}) = 0.302 \text{ barns/steradian.}$$

(It should be noted that the Rutherford formula does not give either this magnitude or angular dependence for carbon-12 at this energy.)

Solving Eq. (2) for ϵ_g and using these values we get

$$\epsilon_g = 3.98 \times 10^{-15} \text{ ev cm}^2\text{/atom of carbon.}$$

This result agrees very well with the independently measured value of 4.0×10^{-15} ev cm^2/atom of carbon obtained by Fuchs and Whaling.[15] The agreement indeed must be fortuitous because of the uncertainties involved in the cross section extrapolation and the value of the incident energy used, which could be in error by 5%.

Conclusions and Comparison with Theory

In order to apply Brandt's theory[17] to the results of this experiment we write the stopping power of graphite or of diamond (in Mev/g cm^{-2}) as:

$$-\frac{dE}{dx_i} = \frac{0.3072Z}{\beta^2 M}\left\{\ln\frac{2m_0C^2\beta^2}{I_0(Z)} - \left(\frac{\delta_1}{2}\right)_i - \left(\frac{\delta_2}{2}\right)_i\right\}, \quad (6)$$

where $Z = 6$, $M = 12$ for carbon and $i = g$ for graphite or d for diamond. Also

$$\left(\frac{\delta_1}{2}\right)_i = \frac{N}{2Z}\ln\frac{\alpha_0}{\alpha_i} \quad \text{and} \quad \left(\frac{\delta_2}{2}\right)_i = \frac{4\pi}{3}\frac{AN}{MZ}\rho_i\alpha_i \quad (7)$$

are the valence and polarization corrections, respectively. Here $N = 4$ (the number of valence electrons in carbon), ρ_i = density, α_0 = the atomic polarizability of carbon, α_i = the polarizabilities of graphite and diamond, and A = Avogadro's number.

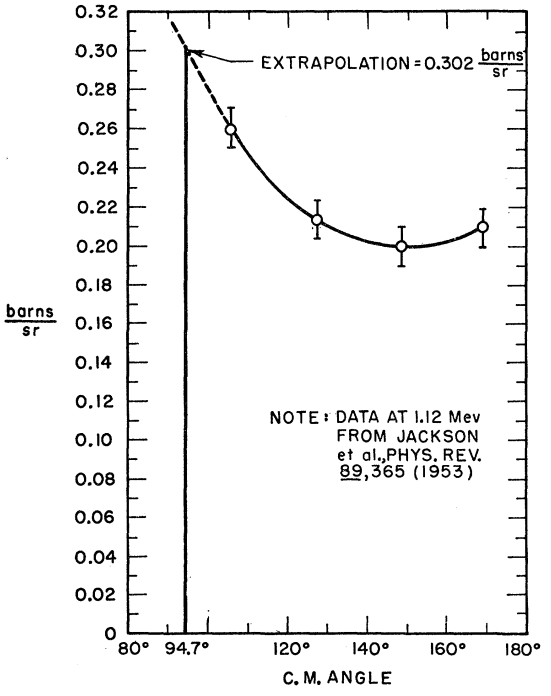

FIG. 6. Extrapolation of carbon scattering cross section.

[13] This is in agreement with an estimate of the maximum possible adsorption of N_2 in the graphite as extrapolated from the curve in Landolt-Börnstein (sixth edition, Vol. II, Pt. 3, p. 512) for adsorption of N_2 in coconut-shell charcoal. This extrapolation gave an upper limit of 7×10^{-5} cm^3 of N_2 at STP/g for adsorption at 0.1 micron pressure and 0°C. Curves from the same reference for H_2 adsorption showed much lower values than these.

[14] Sylvan Rubin (private communication).

[15] R. Fuchs and W. Whaling, California Institute of Technology Report (unpublished).

[16] H. Jackson *et al.* Phys. Rev. 89, 365 (1953).

[17] W. Brandt, du Pont Radiation Physics Laboratory Report (unpublished).

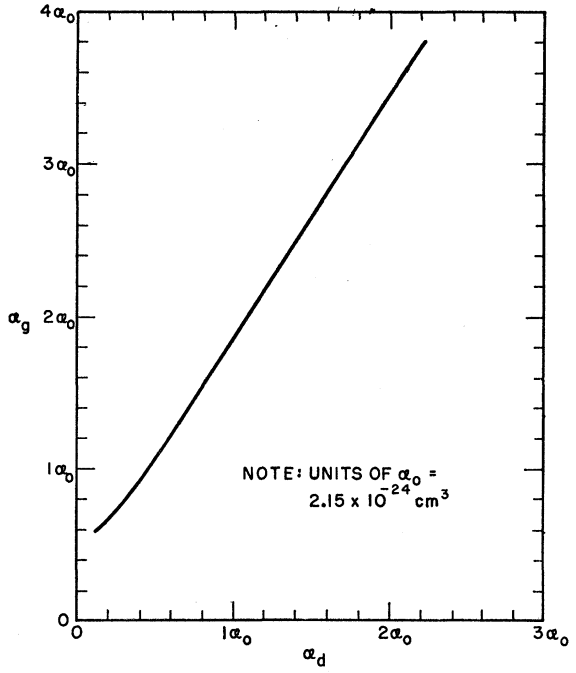

FIG. 7. α_g vs α_d in units of α_0 for $\epsilon_g/\epsilon_d=1.06$.

Brandt[17] gives for carbon $I_0(Z)=60$ ev and

$$\alpha_0=2.15\times10^{-24}\ \text{cm}^3.$$

The measured ratio of the stopping powers is

$$\left(\frac{dE}{dx}\right)_g\div\left(\frac{dE}{dx}\right)_d=1.0604\pm0.0090.$$

Solving for the polarizabilities α_g of graphite and α_d of diamond by numerical and graphical methods using

$\rho_g=2.25$ g/cm³ (theoretical density of graphite),

$\rho_d=3.51$ g/cm³ (theoretical density of diamond),

$\beta^2=2.41\times10^{-3}$ for 1.1-Mev protons,

we obtain the curve shown in Fig. 7 for α_g vs α_d for values of α_g from $0.59\alpha_0$ to $4\alpha_0$. The analytical expression for this curve is

$$\alpha_g=1.60\alpha_d+0.22\alpha_0 \quad \text{for} \quad \alpha_g>\alpha_0.$$

In reference 7 Brandt gives $\alpha_g=0.59\alpha_0$, for which we obtain $\alpha_g/\alpha_d=4.9$ from the curve, the experimental ratio of the polarizabilities of graphite and diamond, based upon theoretical densities of perfect crystals.

The author is indebted to Werner Brandt for suggesting[18] that the actual measured density of the graphite should be used in the above calculation instead of the theoretical density. From the above experiment, he gets two roots for the value of α_g/α_d:

$$1.55\pm0.4 \quad \text{and} \quad 2.3\pm0.4,$$

using the mean of the measured density, $\rho_g=1.68$ g/cm³. His independent estimate of α_g/α_d prior to this experiment was

$$(\alpha_g/\alpha_d)_{\text{theoretical}}=1.5,$$

agreeing well with the first root.

In the author's opinion it would be a most interesting result of the experiment if the stopping power of solids is better described by a theory which uses the macroscopic density rather than the expected microscopic values of the parameter.

An actual solution of both equations for α_g and α_d in terms of the absolute stopping powers ϵ_g and ϵ_d cannot be made, because Eq. (6) will not give a real solution for the measured values of ϵ_i. This is not surprising, since the determination of the absolute stopping powers is probably uncertain by at least 5%, far more than the values of the smaller terms in Eq. (6).

Theory predicts that stopping power will be isotropic even in perfect crystals. This assumption was not tested in this experiment, but since a large effect due to crystal structure was observed it is possible that the stopping power may depend somewhat on crystal orientation. Further experiments should investigate this point since results of recent experiments elsewhere show that sputtering from crystals exhibits strong anisotropy.[19]

Qualitatively, the major difference between graphite and diamond which could affect stopping power is in the number of energy levels in the solid which are available for excitation. Compared with diamond, graphite has many more low-lying levels which contribute to energy loss by distant collisions.

ACKNOWLEDGMENTS

Thanks are due to the SRI Physical Sciences Division Research Committee, which sponsored this work, to O. Preston and A. Nieman of the SRI metallurgy department for providing the pyrolytic graphite, and to C. Blackmon for assistance during the experiment. In particular the author is indebted to Dr. Sylvan Rubin of SRI, who provided the basic idea behind the experiment and whose continued advice and encouragement were essential to the completion of the experiment, and to Dr. Werner Brandt of Du Pont, whose theoretical opinions have been very helpful in the interpretation of the results.

APPENDIX

Derivation of Equation (2) for Yield of Scattered Protons from a Thick Target

Notation:

E_1=proton energy (Mev) before scattering,

E_2=proton energy (Mev) after scattering,

d_1=path of proton in target (cm) before scattering,

[18] W. Brandt (private communication).

[19] P. Rol, J. Fluit, F. Viehbock, and M. deJong, *Fourth International Conference on Ionization Phenomena in Gases, Uppsala, Sweden* (North Holland Publishing Company, Amsterdam, 1960).

d_2 = path of proton in target (cm) after scattering,
ϵ_1 = stopping power [(Mev−cm²)/atom] of target for protons of energy E_1,
ϵ_2 = stopping power [(Mev−cm²)/atom] of target for protons of energy E_2,
n = number of atoms per cm³ in target,
$1/R_s$ = fractional momentum resolution of magnetic spectrometer; $\Delta P/P = 1/R_s$,
h = depth into target (cm) at which scattering takes place,
α = angle of incident beam with normal to target surface (rad),
$\theta-\alpha$ = angle of scattered beam with normal to target surface (rad),
σ = differential scattering cross section for target atoms at angle θ in the laboratory system and at energy E_1 in the laboratory system (cm²/atom sr),
q = number of protons incident on the target,
Ω = acceptance solid angle (sr) of the magnetic spectrometer,
C = number of scattered protons accepted by spectrometer.

See Fig. 1 for the scattering geometry.
Only elastic scattering is considered, for which

$$E_2 = kE_1, \tag{1}$$

and k is known from the kinematics and known mass of the scattering nucleus. (The spectrometer accepts only protons in the interval from E_2 to $E_2-\Delta E_2$.) Protons lose ΔE_1 before scattering, change in energy by k, then lose $\Delta E_2'$ after scattering. Therefore

$$E_2-\Delta E_2 = k(E_1-\Delta E_1)-\Delta E_2', \tag{2}$$

and

$$\Delta E_1 = n\epsilon_1 d_1, \tag{3}$$

$$\Delta E_2' = n\epsilon_2 d_2, \tag{4}$$

from which

$$\Delta E_2 = k\Delta E_1+\Delta E_2' \tag{5}$$

is derivable. Since the fractional momentum resolution of the magnetic spectrometer is $1/R_s=\Delta P/P$, the fractional energy resolution is

$$\Delta E_2/E_2 = 2/R_s; \tag{6}$$

hence

$$\frac{2}{R_s}=\frac{k\Delta E_1+\Delta E_2'}{kE_1}=\frac{\Delta E_1+\Delta E_2'/k}{E_1}, \tag{7}$$

and by further substitution

$$\frac{2E_1}{R_s}=n\left[\epsilon_1 d_1+\frac{\epsilon_2}{k}d_2\right].$$

From Fig. 1,

$$d_2 = d_1\frac{\cos\theta}{\cos(\theta-\alpha)};$$

consequently

$$d_1=\frac{2E_1}{nR_s}\left[\epsilon_1+\frac{\cos\alpha}{\cos(\theta-\alpha)}\frac{\epsilon_2}{k}\right]^{-1}. \tag{8}$$

The yield of scattered protons is

$$C = \sigma nqd_1\Omega,$$

so that

$$C=\left(\frac{2E_1\sigma q\Omega}{R_s}\right)\left[\epsilon_1+\frac{\cos\alpha}{\cos(\theta-\alpha)}\frac{\epsilon_2}{k}\right]^{-1}, \tag{9}$$

which is Eq. (2) of the text.